

PERIODIC ORBITS AROUND THE TRIANGULAR POINTS WITH PROLATE PRIMARIES

Nihad ABD EL MOTELP¹, Mohamed RADWAN²

¹ Astronomy Department, National Research Institute of Astronomy
 and Geophysics (NRIAG), Cairo, Egypt

² Astronomy and Space Science Department, Faculty of Science,
 Cairo University, Egypt

e-mails: nihad.saad@nriag.sci.eg, mradwan@sci.cu.edu.eg

ABSTRACT. Periodic orbits play a fundamental role in the study and deep understanding of the behavior of dynamical systems. In the current work, we investigated the periodic orbits around the triangular libration points of the restricted three-body problem. The equations of motion of the restricted problem are presented when both primaries are prolate triaxial. Periodic orbits around the triangular points are obtained and then illustrated graphically for some selected initial conditions and for the entire domain of the mass ratio μ , as well. The eccentricities of the periodic orbits are obtained and then represented graphically. It is observed that the periodic orbits about the triangular stationary points are elliptical, and the frequencies of short and long orbits of the periodic motion are influenced by the shape of the primary bodies. Furthermore, we found that the perturbing forces influence the period, the orientation, and the eccentricities of the short and long periodic orbits.

Keywords: restricted three-body problem, triangular points, prolate triaxial, periodic orbits

1. INTRODUCTION

The restricted problem of three bodies is considered one of the most important and famous problems of dynamics. This is due to its wide extremely important applications in the field of space dynamics, it describes accurately many real-world problems. In the restricted three-body problem, a body of negligible mass moves under the influence of the gravitational fields of two massive bodies. These two primary bodies rotate in circular or elliptic orbits about their common center of mass. Having negligible mass, the force exerted on the two primaries by the third body may be neglected.

The dynamic system of the restricted three-body problem is characterized by the presence of five equilibrium points. In this system, the gravitational and the centrifugal forces on a spacecraft mass cancel each other out. These fixed points are called equilibrium points. Three of these points are collinear, and two of them are triangular. These points rotate at the same frequency as the massive bodies, and thus the spacecraft mass's position relative to the primaries is constant. This makes them very important for research and space operations (Marsola et al., 2021); (Reiff et al., 2022).



Furthermore, the periodic orbits around these equilibrium points acquired great attention and interest due to the crucial need for space orbits in the proximity of one of the collinear or triangular equilibrium points, (Abd El-Salam, 2019). Also, periodic orbits can be utilized to explore small solar system bodies, including comets and asteroids.

Different methodologies have been used to address the restricted three-body problem. In general, quantitative methods, either analytical or numerical, give precise and accurate information on the evolution of differential systems. However, this information is usually limited to the solution of interest and to a small vicinity. Also, in most cases, the accuracy decreases as time increases. In the current work, to obtain the required accuracy of the actual space mission orbit, we combined an analytical perturbed solution with a qualitative method. This technique gives partial but also rigorously demonstrated properties that are valid at least for long periods of time. Moreover, it deals with questions of existence, integrals of motion, uniqueness, periodic orbits, stability, etc.

Over the years, many researchers have investigated the issue of the restricted problem from various aspects, such as locations, stability of stationary points, and the periodic orbits, to mention some (Abouelmagd et al., 2016) (Burgos et al., 2019) (Pathak et al., 2019).

Recently, Poddar and Sharma, (2021) studied the equations of motion for the problem, which are regularized in the neighborhood of one of the finite masses. Further, the authors studied the existence of periodic orbits in a three-dimensional coordinate system when the reduced mass equals zero. Radwan and Abd El Motelp,(2021) investigated the linear stability of the restricted three-body problem when both of the massive primaries are triaxial. Also, they studied the periodic orbits in the vicinity of the triangular points. The authors showed that the shape of periodic orbits changed because of the triaxiality of the primary bodies. (Alrebdi et al., 2022) investigated how the mass ratio μ and the transition parameter influence the stationary points of the pseudo-Newtonian planar circular restricted problem. The authors also, showed how these parameters influence the networks of simple symmetric periodic orbits.

In the current work, we study the periodic orbits around the triangular points in the elliptic restricted three-body problem frame of work. To obtain a more realistic representation, the problem is generalized in the sense that bigger and smaller primaries are modeled as prolate spheroids. Also, we study in detail the variations in the angular frequencies for the long and short periodic orbits due to the shape of the primaries. Moreover, we compute explicit expressions for the eccentricities of the ellipses and determine the orientations of the principal axes for the ellipses that represent periodic orbits.

2. MOTIVATIONS

It is well known in the field of space science that most celestial bodies are often irregular in shape. In the original version of the restricted problem, the massive primaries are supposed to be spherical and symmetrical bodies (Szebehely, 1967). However, when studying various problems, the irregular shapes of these bodies must be taken into account in order to obtain highly efficient solutions. In some cases, considering the two primaries as point mass is not sufficient to describe the dynamic problem.

Over the past decades, several modifications have been proposed to include different additional parameters in the effective potential, such as the oblateness, the triaxiality, or the radiation of the two massive primaries (AbdulRaheem and Singh, 2008) (Beatty and Chaikin, 1999) (Radwan and Abd El Motelp, 2021) (Sharma and Subba, 1975) (Zahra et. al, 2017), and (Zotos, 2020). The mentioned reasons motivated us to study the dynamics of the problem under the influence of the real shape of the primaries. Furthermore, periodic orbits give more insights into a better

understanding of the complex dynamical system of the restricted problem. Therefore, the crucial need for periodic orbits motivated us to study these orbits when both primaries are prolate spheroids.

3. DYNAMICAL MODEL

The current dynamical system contains an infinitesimal mass that rotates in the orbital plane of the two massive bodies, the primary m_1 and the secondary mass m_2 . The third infinitesimal one is considered to act as a test particle while the two primaries are prolate triaxial and circulate about their common centre of mass. The motion of the infinitesimal body doesn't have any dynamic impact on the motion of the main bodies, due to its insignificant mass. In order to remove the time dependence from the equations of motion, it is better to use a synodic-rotating frame that rotates with constant angular velocity about the z-axis. The origin of the reference frame is centered at the barycentre of the system, and the x-axis lies on the line joining the two primary bodies. For convenience, we use a units system where the constant of gravity G and the distance between the centers of the two primaries are both equal to unity. Utilizing the reduced mass $\mu = \frac{m_1}{m_1+m_2}$, we can express the dimensionless masses of the two primaries as $m_1 = 1 - \mu$ and $m_2 = \mu$. Following the notations of Szebehely, (1967), the equations of motion of the tiny object in the dimensionless rotating-synodic frame are given by

$$\ddot{x} - 2n\dot{y} = \frac{\partial U}{\partial x}, \quad \ddot{y} + 2n\dot{x} = \frac{\partial U}{\partial y}, \quad (1)$$

where the amended potential function U can be written as

$$U = \frac{n^2}{2} (x^2 + y^2) + \frac{(1-\mu)}{r_1} \left(1 + \frac{A_\sigma}{2r_1^2}\right) + \frac{\mu}{r_2} \left(1 + \frac{A_\gamma}{2r_2^2}\right) \quad (2)$$

and

$$\begin{aligned} r_1 &= \sqrt{(x+\mu)^2 + y^2}, \\ r_2 &= \sqrt{(x+\mu-1)^2 + y^2}, \end{aligned} \quad (3)$$

The perturbed mean motion of the primaries is given by

$$n = \sqrt{\frac{1}{a} \left(1 + \frac{3}{2} (A_\gamma + A_\sigma) (1 + e^2)\right)}, \quad (4)$$

where r_1 and r_2 are the distances of the two massive bodies from the infinitesimal third body. A_γ and A_σ represent the prolateness coefficients. a and e are the semi-major axis and eccentricity of either primary, respectively.

4. THE LOCATIONS OF THE TRIANGULAR POINTS

The locations of the equilibrium triangular points L_4 and L_5 can be obtained by setting all relative velocity and relative acceleration components equal to zero and solving the resulting system of equations $U_x = U_y = 0$. The first derivatives of the potential function can be written as

$$\begin{aligned} U_x &= n^2 x - \frac{(3A_\gamma + 2r_2^2)\mu(-1+x+\mu)}{2r_2^5} - (-1+\mu) \\ &\quad (x+\mu) \left[\frac{3A_\sigma}{2r_1^5} - \frac{1}{r_1^3} \right] \end{aligned} \quad (5)$$

$$U_y = y \left[n^2 + (-1 + \mu) \left(\frac{3 A_\sigma}{2 r_1^5} + \frac{1}{r_1^3} \right) - \mu \left(\frac{3 A_\gamma}{2 r_2^5} + \frac{1}{r_2^3} \right) \right] \quad (6)$$

Since the perturbations considered in the present work are small, i.e., the prolateness coefficients are much smaller than unity, therefore, we can ignore its values (i.e., $r_1 = r_2 = 1$). Then it may be reasonable here to suppose that the locations of the triangular points $L_{4,5}$ are the same as given by classical restricted problem but perturbed by terms $\delta_1, \delta_2 = \mathcal{O}(A_\gamma, A_\sigma)$. In this case, the solution of the classical restricted problem can be written as

$$r_i = 1 + \delta_i, \quad \delta_i \ll 1, \quad (i = 1, 2). \quad (7)$$

Using equations (5) and (6) and solving for x and y up to order one in the involved small quantities δ_1, δ_2 , we obtain

$$x = \frac{1}{2} (2 \delta_1 - 2 \delta_2 - 2 \mu + 1), \quad y = \pm \frac{\sqrt{3}}{2} \sqrt{1 + \frac{4}{3} (\delta_1 + \delta_2)}, \quad (8)$$

Substituting the values of x, y, r_1 , and r_2 into equations (5) and (6), and expanding the resulting equations, we can retained only first order terms in δ_1, δ_2 . Therefore, we get

$$\begin{aligned} \delta_1 &= \frac{1}{3} - \frac{1}{3a} \left(1 + e^2 + \frac{3}{2} A_\gamma (1 + e^2) + A_\sigma (1 + e^2) \right), \\ \delta_2 &= \frac{1}{3} - \frac{1}{3a} \left(1 + e^2 + \frac{3}{2} A_\sigma (1 + e^2) + A_\gamma (1 + e^2) \right). \end{aligned} \quad (9)$$

Substituting the values of δ_1, δ_2 into equations (8) yields the coordinates of the equilibrium triangular points

$$\begin{aligned} x &= \frac{1}{2} - \mu - \frac{A_\gamma}{6a} (1 + e^2) + \frac{A_\sigma}{6a} (1 + e^2), \\ y &= \pm \frac{\sqrt{3}}{18} \left[13 - (1 + e^2) \left[\frac{4}{a} + \frac{5}{a} (A_\gamma + A_\sigma) \right] \right] \end{aligned} \quad (10)$$

Note that if we ignore the involved perturbations, equations (10) will lead to the corresponding classical one.

5. PERIODIC ORBITS

It is well known that periodic orbits are of great importance, and they represent the backbone of studying the behavior of dynamic systems in the field of celestial mechanics. Let the locations of the equilibrium points be given as $(x_{L_{4,5}}, y_{L_{4,5}})$. Let us give the equilibrium points a small displacement (ξ_0, η_0) , i.e., $\xi_0, \eta_0 \ll 1$. We have

$$x = x_{L_{4,5}} + \xi_0, \quad y = y_{L_{4,5}} + \eta_0 \quad (11)$$

Then the corresponding characteristic equation of the current problem is given by Szebehely, (1967)

$$\lambda^4 + (4n^2 - U_{xx}^{L_{4,5}} - U_{yy}^{L_{4,5}}) \lambda^2 + U_{xx}^{L_{4,5}} U_{yy}^{L_{4,5}} - (U_{xy}^{L_{4,5}})^2 = 0 \quad (12)$$

where

$$\begin{aligned} U_{xx}^{L_{4,5}} &= \frac{-1}{2} + \frac{5}{4a} (1 + e^2) + A_\sigma \left[\frac{-3}{2} + \frac{33}{8a} (1 + e^2) + \frac{3\mu}{2} - \frac{11\mu}{4a} (1 + e^2) \right] \\ &+ A_\gamma \left[\frac{11}{8a} (1 + e^2) - \frac{3\mu}{2} + -\frac{11\mu}{4a} (1 + e^2) \right], \end{aligned} \quad (13)$$

$$U_{yy}^{L_{4,5}} = \frac{1}{2} + \frac{7}{4a} (1 + e^2) + A_\sigma \left[\frac{-3}{2} + \frac{59}{8a} (1 + e^2) + \frac{3\mu}{2} - \frac{17\mu}{4a} (1 + e^2) \right] + A_\gamma \left[\frac{25}{8a} (1 + e^2) - \frac{3\mu}{2} + \frac{17\mu}{4a} (1 + e^2) \right], \quad (14)$$

and

$$U_{xy}^{L_{4,5}} = \frac{\sqrt{3}}{3} \left[\frac{-1}{2} + \frac{11}{4a} (1 + e^2) + \left(1 - \frac{11}{2a} (1 + e^2) \right) \mu + A_\gamma \left(\frac{29}{8a} (1 + e^2) + \left(5 - \frac{35}{2a} (1 + e^2) \mu \right) \right) + A_\sigma \left(-5 + \frac{111}{8a} (1 + e^2) + \left(5 - \frac{35}{2a} (1 + e^2) \mu \right) \right) \right]. \quad (15)$$

$U_{xx}^{L_{4,5}}$, $U_{yy}^{L_{4,5}}$, and $U_{xy}^{L_{4,5}}$ are the second partial derivatives of the amended potential function evaluated at the triangular points. The roots of the characteristic polynomial λ_i , of the present system, in the range $0 \leq \mu \leq \mu_{critical}$, are purely imaginary. Therefore, the motion about the triangular equilibrium points $L_{4,5}$ is stable and composed of two harmonic motions governed by the variations

$$\begin{aligned} \xi &= C_1 \cos s_1 t + D_1 \sin s_1 t + C_2 \cos s_2 t + D_2 \sin s_2 t, \\ \eta &= \bar{C}_1 \cos s_1 t + \bar{D}_1 \sin s_1 t + \bar{C}_2 \cos s_2 t + \bar{D}_2 \sin s_2 t \end{aligned} \quad (16)$$

where s_1, s_2 are the frequencies for long and short periodic orbits, respectively. The coefficients C_1, D_1, \bar{C}_1 , and \bar{D}_1 are the long periodic terms, while the coefficients C_2, D_2, \bar{C}_2 , and \bar{D}_2 are the short periodic terms. The frequencies s_1 , and s_2 are given up to order μ^2 as

$$\begin{aligned} s_1 &= \frac{1}{3226944} \left[98 \frac{\sqrt{21}}{a} (1 + e^2) (-5488 + 47432 \mu + 157542 \mu^2) - 7 A_\sigma \left(16464 \left(-42 + \frac{25 \sqrt{21}}{a} \right) - 392 \left(-1764 + 2573 \frac{\sqrt{21}}{a} \right) \mu + 7324086 \frac{\sqrt{21}}{a} \mu^2 + \frac{\sqrt{21}}{a} e^2 \left(411600 - 1008616 \mu + 7324086 \mu^2 \right) \right) + 7 A_\gamma \left(-71344 \frac{\sqrt{21}}{a} + 392 \left(1764 + 8339 \frac{\sqrt{21}}{a} \right) \mu + 21978726 \frac{\sqrt{21}}{a} \mu^2 + \frac{\sqrt{21}}{a} e^2 \left(-71344 + 3268888 \mu + 21978726 \mu^2 \right) \right) - 6 a \sqrt{21} (-1 + e^2) \left(A_\sigma (44688 + 165592 \mu - 13661634 \mu^2) + 14 \left(-784 + 1624 \mu + 128330 \mu^2 + A_\gamma \left(-2352 - 429352 \mu + 2817990 \mu^2 \right) + 14 \left[8 \left(686 \left(4 \sqrt{21} + \frac{21}{a} \right) + \frac{14406}{a} e^2 + 8624 \sqrt{21} \mu + 168399 \sqrt{21} \mu^2 - A_\sigma \left[-85456 \sqrt{21} + \frac{633864}{a} + 56 \left(9335 \sqrt{21} - 14406 \frac{\mu}{a} \right) + 9481146 \sqrt{21} \mu^2 - \frac{57624}{a} e^2 (-11 + 14 \mu) \right] + 8 A_\gamma \left(147 \left(-8 \sqrt{21} + \frac{147}{a} \right) - 14 \left(64 \sqrt{21} + \frac{7203}{a} \right) \mu + 1077477 \sqrt{21} \mu^2 - \frac{7203}{a} e^2 (-3 + 14 \mu) \right) \right] \right]. \quad (17) \end{aligned}$$

and

$$\begin{aligned}
s_2 = & \frac{1}{3226944} \left[-98 \frac{\sqrt{21}}{a} (1 + e^2) (-5488 + 47432 \mu + 157542 \mu^2) + 7 A_\sigma \left(16464 \right. \right. \\
& \left. \left(42 + \frac{25 \sqrt{21}}{a} \right) - 392 \left(1764 + 2573 \frac{\sqrt{21}}{a} \right) \mu + 7324086 \frac{\sqrt{21}}{a} \mu^2 + \frac{\sqrt{21}}{a} e^2 \right. \\
& \left. (411600 - 1008616 \mu + 7324086 \mu^2) - 7 A_\gamma \left(-71344 \frac{\sqrt{21}}{a} + 392 \left(-1764 + 8339 \right. \right. \right. \\
& \left. \left. \frac{\sqrt{21}}{a} \right) \mu + 21978726 \frac{\sqrt{21}}{a} \mu^2 + \frac{\sqrt{21}}{a} e^2 (-71344 + 3268888 \mu + 21978726 \mu^2) \right) \\
& + 6 a \sqrt{21} (-1 + e^2) \left(A_\sigma (44688 + 165592 \mu - 13661634 \mu^2) + 14 \left(-784 + 1624 \mu \right. \right. \\
& \left. \left. + 128330 \mu^2 \right) + A_\gamma (-2352 - 429352 \mu + 2817990 \mu^2) \right) - 14 \left[8 \left(686 \left(4 \sqrt{21} - \frac{21}{a} \right) \right. \right. \\
& \left. \left. - \frac{14406}{a} e^2 + 8624 \sqrt{21} \mu + 168399 \sqrt{21} \mu^2 - A_\sigma \left[-392 \left(218 \sqrt{21} + \frac{1617}{a} \right) \right. \right. \right. \\
& \left. \left. + 56 \left(9335 \sqrt{21} + 14406 \frac{1}{a} \right) \mu + 9481146 \sqrt{21} \mu^2 + \frac{57624}{a} e^2 (-11 + 14 \mu) \right] \right. \\
& \left. + 8 A_\gamma \left(-147 \left(8 \sqrt{21} + \frac{147}{a} \right) - 14 \left(64 \sqrt{21} - 7203 \frac{1}{a} \right) \mu + 1077477 \sqrt{21} \right. \right. \\
& \left. \left. \mu^2 + \frac{7203}{a} e^2 (-3 + 14 \mu) \right) \right].
\end{aligned} \tag{18}$$

It can be seen from equations (17) and (18) that the frequencies of the orbit of both short and long periodic motions are affected by the prolateness coefficients of the primaries, the mass ratio, the semi-major axis a , and the eccentricity e . as can be seen in the following illustrative graphs:

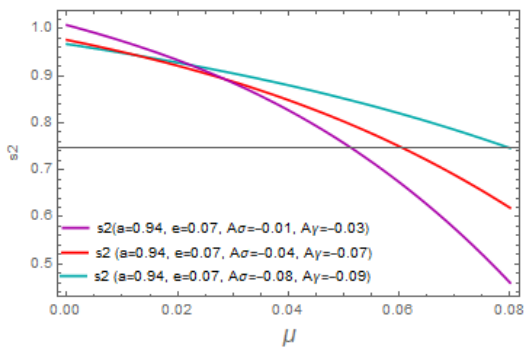


Figure 1.a. The variation of short-period frequency versus mass parameter μ for different values of the plorate triaxiality

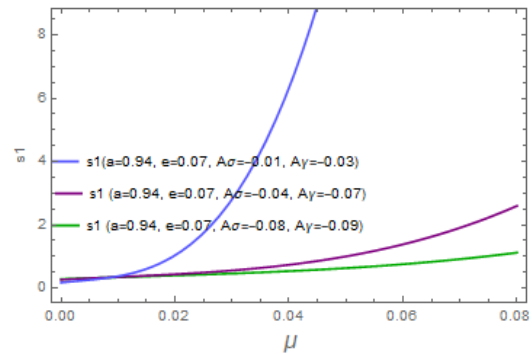


Figure 1.b. The variation of long-period frequency versus mass parameter μ for different values of the plorate triaxiality parameter

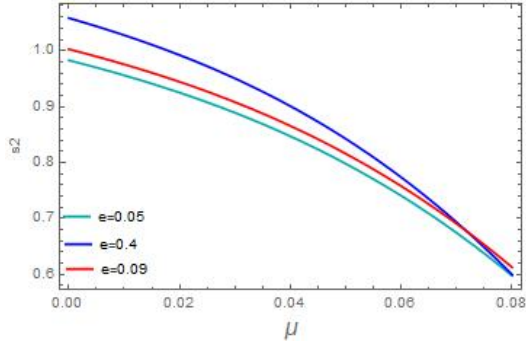


Figure 2.a. Eccentricity effect on the short-period frequency

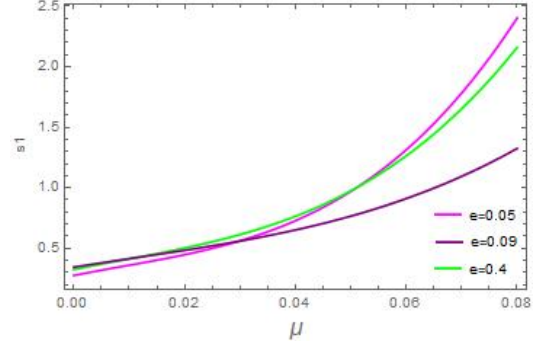


Figure 2.b. Eccentricity effect on the long-period frequency

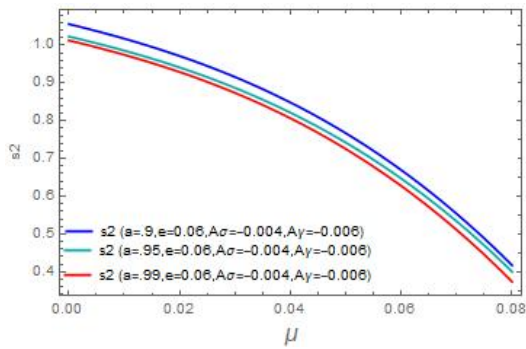


Figure 3.a. The variations of s_2 versus mass parameter μ for different values of semi-major axis ($a = 0.90, 0.95, 0.99$), with fixed values of $A_\sigma = -0.004$, $A_\gamma = -0.006$, and $e = 0.06$

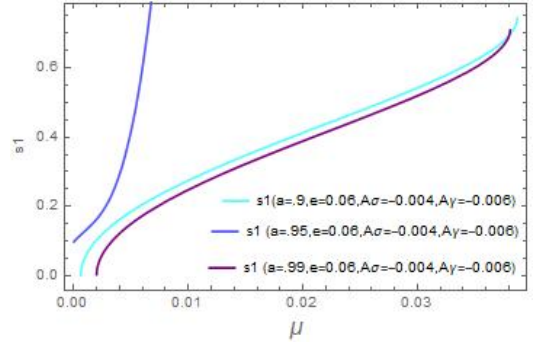


Figure 3.b. The variations of s_1 versus the mass parameter μ for different values of the semimajor axis ($a = 0.90, 0.95, 0.99$), with fixed prolateness triaxiality coefficients $A_\gamma = -0.006$, $A_\sigma = -0.004$, and $e = 0.06$

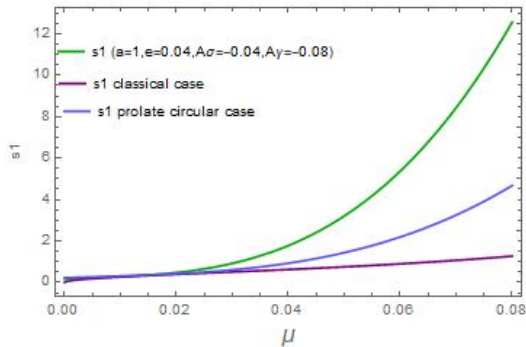


Figure 4.a. Comparing the long-period frequency for some selected cases with the classical case

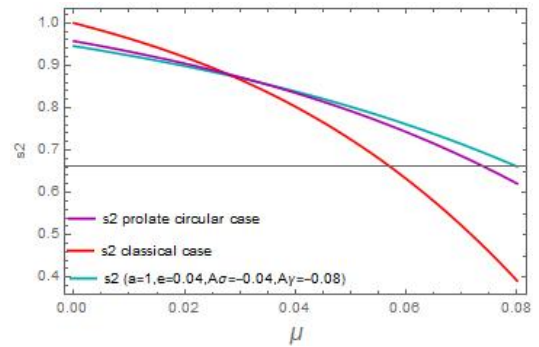


Figure 4.b. Comparing the short-period frequency for some selected cases with the classical case

Figs. 1a and 1b illustrate the variations of the two frequencies s_2 and s_1 for different values of the prolateness coefficients A_σ , A_γ and $e = 0.07, a = 0.94$. Figs. 2a and 2b depict the variations of the short- and long-periodic frequencies s_2 and s_1 with the mass ratio μ for different values of the eccentricity of either primary ($e = 0.05, 0.09, 0.4$, $A_\sigma = -0.06$, $A_\gamma = -0.04$, and $a = 0.94$). It is observed that, in the above mentioned curves, the short-period frequency s_2 is a decreasing function, while the long-period frequency s_1 is an increasing one. Figs. 3a and 3b depict the variations of the long- ,and short periodic frequencies s_1 and s_2 with the mass

parameter μ , for different values of the semi-major axis ($a = 0.90, 0.95, 0.99$). The figures show that the long period frequency, s_1 , is an increasing function, while the short- period frequency, s_2 is a decreasing function. Figs. 4a, and 4b depict the variations in angular frequencies s_1 , and s_2 under the effect of the perturbation considered in comparison with the classical case. It can be seen from both figures the effect of the perturbing forces on the behavior of the curves representing the angular frequencies. The perturbing forces cause these curves to depart from the classical case.

6. ELLIPTICAL ORBITS

The expansion of the amended potential function U about the triangular equilibrium points $L_{4,5}$ is

$$U = U^{L_{4,5}} + U_{xx}^{L_{4,5}} \xi^2 + U_{yy}^{L_{4,5}} \eta^2 + U_{xy}^{L_{4,5}} \xi \eta + \mathcal{O}(3) \quad (19)$$

As we can see equation (19) is quadratic, thus, the periodic orbits around the libration points $L_{4,5}$ are elliptical, since the Hessian $U_{xx}U_{yy} - U_{xy}^2 > 0$.

6.1. Orientation of the principal axes of the ellipses

Equation (19) can be expressed in the form

$$U = L \xi^2 + M \xi \eta + N \eta^2 + U_0 \quad (20)$$

where

$$L = \frac{-1}{4} + \frac{5}{8a} + \frac{5e^2}{8a} + A_\sigma \left(-\frac{3}{4} + \frac{33}{16a} (1+e^2) + \mu \left(\frac{3}{4} - \frac{11}{8a} (1+e^2) \right) \right) + A_\gamma \left(\frac{11}{16} (1+e^2) + \left(\frac{-3}{4} + \mu \frac{11}{16a} (1+e^2) \right) \right), \quad (21)$$

$$M = \frac{\sqrt{3}}{3} \left[\frac{-1}{2} + \frac{11}{4a} (1+e^2) + \mu \left(1 - \frac{11}{2a} (1+e^2) \right) + A_\gamma \left(\frac{29}{8a} (1+e^2) + \left(5 - \frac{35}{2a} (1+e^2) \right) \mu \right) + A_\sigma \left(-5 + \frac{111}{8a} (1+e^2) + \left(5 - \frac{35}{2a} (1+e^2) \right) \right) \right], \quad (22)$$

$$N = \frac{1}{4} + \frac{7}{8a} (1+e^2) + A_\sigma \left(\frac{-3}{4} + \frac{59}{16a} (1+e^2) \right) + \mu \left(\frac{3}{4} - \frac{17}{8a} (1+e^2) \right) + A_\gamma \left(\frac{25}{16a} (1+e^2) + \mu \left(\frac{-3}{8} + \frac{17}{8a} (1+e^2) \right) \right), \quad (23)$$

and

$$U_0 = \frac{2}{3} - \frac{5}{27a^2} + \frac{59}{54a} + \left(\frac{-10}{27a^2} + \frac{59}{54a} \right) e^2 - \frac{\mu}{2a} (1+e^2) + \frac{\mu^2}{2a} (1+e^2) + A_\sigma \left(\frac{-23}{54a^2} + \frac{71}{36a} + e^2 \left(\frac{-23}{27a^2} + \frac{71}{36a} \right) - \left(\frac{1}{6a^2} + \frac{13}{12a} + \left(\frac{1}{3a^2} + \frac{13}{12a} \right) e^2 \right) \mu + \frac{3}{4a} (1+e^2) \mu^2 \right) + A_\gamma \left(\frac{-16}{27a^2} + \frac{59}{36a} + e^2 \left(\frac{-32}{27a^2} + \frac{59}{36a} \right) + \left(\frac{1}{6a^2} - \frac{5}{12a} + \left(\frac{1}{3a^2} - \frac{5}{12a} \right) e^2 \right) \mu + \frac{3}{4a} (1+e^2) \mu^2 \right) \quad (24)$$

$$\xi = \bar{\xi} \cos \theta - \bar{\eta} \sin \theta, \quad \eta = \bar{\xi} \sin \theta + \bar{\eta} \cos \theta. \quad (25)$$

Hence, the new form of equation (20), is given as

$$U = \bar{L} \bar{\xi}^2 + \bar{N} \bar{\eta}^2 + \bar{U}_0$$

where \bar{L} , \bar{N} , and \bar{U}_0 are new modified quantities. It is easily seen from equation (20) that the periodic orbits around the triangular points $L_{4,5}$ are elliptical. Setting the term that contains $\bar{\eta} \bar{\xi}$ equal to zero, we have

$$\tan 2\theta = \frac{2 U_{xy}}{U_{xx} - U_{yy}}$$

$$\tan 2\theta = \pm \frac{\sqrt{3}}{3 [4a + (1 + e^2) (2 + A_\sigma (13 - 6\mu) + A_\gamma (7 + 6\mu))] \left[(1 + e^2) \left[-22 - 29 A_\gamma - 111 A_\sigma + \mu (44 + 140 (A_\gamma + A_\sigma)) \right] + 4a \left[1 + 10 A_\sigma - 10\mu \left(\frac{1}{5} + A_\gamma + A_\sigma \right) \right] \right]} \quad (26)$$

where the plus sign (minus sign) refers to the centre of the ellipse at $L_{4,5}$.

6.2. Eccentricities of the ellipses

In order to obtain the eccentricities of the ellipses, we use the equations Szebehely, (1967)

$$e_1 = (1 - \alpha_1^2)^{\frac{1}{2}} \quad (27)$$

$$e_2 = (1 - \alpha_2^2)^{\frac{1}{2}} \quad (28)$$

and

$$\alpha_i = \frac{2s_i}{s_i^2 + \bar{\lambda}_1} = \frac{s_i^2 + \bar{\lambda}_2}{2s_i} \quad (29)$$

where $\bar{\lambda}_1$ and $\bar{\lambda}_2$ are the roots of the characteristic equation. For $i = 1, 2$, with similar expression for α_2 , we have

$$\begin{aligned}
\alpha_1 = & \frac{-1}{3687936 a} \sqrt{350981 + 229771 \sqrt{\frac{7}{3}}} \left[392 \sqrt{-3 + \sqrt{21}} (1 + e^2) \left(28 \right. \right. \\
& \left. \left(5838 - 1274 \sqrt{21} + (-903 + 197 \sqrt{21}) A_\gamma + (151431 - 3305 \sqrt{21}) A_\sigma \right) + \right. \\
& \left. \left(-4091010 + 892738 \sqrt{21} + (-17969553 + 32921313 \sqrt{21}) A_\gamma + (-8382927 \right. \right. \\
& \left. \left. + 1829311 \sqrt{21}) A_\sigma \right) \mu \right) + 48 \sqrt{-3 + \sqrt{21}} \left(-2415 + 527 \sqrt{21} a^2 (-1 + e^2) \right. \\
& \left. (196 - 798 A_\sigma - 406 \mu - 2957 A_\sigma \mu + A_\gamma (42 + 7667 \mu)) + 21 \sqrt{2} a^{\frac{5}{2}} \right. \\
& \left. (-2 + 3 e^2) \left(336 (74641 \sqrt{3} - 48864 \sqrt{7}) A_\gamma + (10727940055 \sqrt{3} - \right. \right. \\
& \left. \left. 7023085617 \sqrt{7}) A_\gamma \mu + (-152436875591 \sqrt{3} + 99793363029 \sqrt{7}) A_\sigma \mu - \right. \right. \\
& \left. \left. 28 (-1466864 \sqrt{3} + 960288 \sqrt{7} + 67642792 \sqrt{3} A_\sigma \mu - 44282604 \sqrt{7} A_\sigma - \right. \right. \\
& \left. \left. 77585123 \sqrt{3} \mu + 50791389 \sqrt{7} \mu) \right) \right) + 9 \sqrt{2} a^{\frac{7}{2}} (-2 + 5 e^2) \left(A_\gamma \left(29997212 \right. \right. \\
& \left. \left. \sqrt{3} - 19637772 \sqrt{7} + 52699894653 \sqrt{3} \mu - 34500179898 \sqrt{7} \mu \right) + 28 \left(4895492 \right. \right. \\
& \left. \left. \sqrt{3} - 3204852 \sqrt{7} + 422762921 \sqrt{3} \mu - 276763308 \sqrt{7} \mu \right) + A_\sigma \left(-9040057628 \right. \right. \\
& \left. \left. \sqrt{3} + 5918107020 \sqrt{7} - 10526335657773 \sqrt{3} \mu + 689111808570 \sqrt{7} \mu \right) \right) + \\
& 112 \sqrt{-3 + \sqrt{21}} a \left(56 (-2415 + 527 \sqrt{21}) (7 + 22 \mu) + A_\sigma \left(-6938988 + \right. \right. \\
& \left. \left. 1514212 \sqrt{21} + 25797723 \mu - 5629555 \sqrt{21} \mu \right) + A_\gamma \left(405720 - 88536 \sqrt{21} - \right. \right. \\
& \left. \left. 2944578 \mu + 642554 \sqrt{21} \mu \right) \right) + 294 \sqrt{2} a^{\frac{3}{2}} (-2 + e^2) \left(A_\gamma \left(1449028 \sqrt{3} - \right. \right. \\
& \left. \left. 948612 \sqrt{7} + 235533725 \sqrt{3} \mu - 154193028 \sqrt{7} \mu \right) + A_\sigma \left(-50296932 \sqrt{3} \right. \right. \\
& \left. \left. + 32927076 \sqrt{7} - 2310568225 \sqrt{3} \mu + 1512622056 \sqrt{7} \mu \right) + 28 \left(70700 \sqrt{3} - \right. \right. \\
& \left. \left. 46284 \sqrt{7} + 121 (13097 \sqrt{3} - 8574 \sqrt{7}) \mu \right) \right) \left. \right]. \tag{30}
\end{aligned}$$

Equation (26) determines the orientation of the orbits with respect to the rotational coordinate system. It is observed that the orientation of the orbits is affected by the involved perturbations. Equation (27) depicts, for $i = 1, 2$, the eccentricities of the short- and long- periodic orbits around the triangular points $L_{4,5}$.

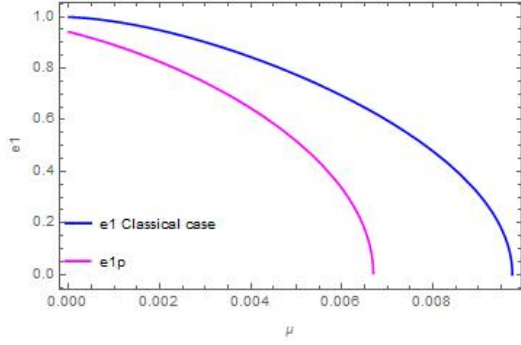


Figure 5.a. Comparing the eccentricity of long period motion in the classical with a selected perturbed case.

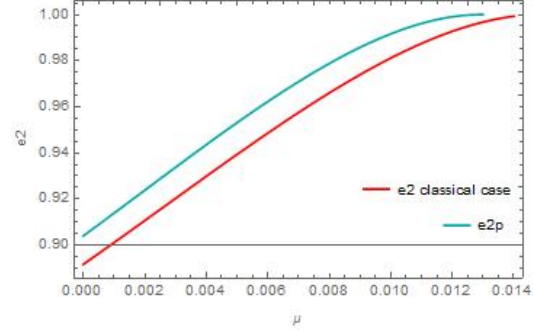


Figure 5.b. Comparing the eccentricity of short-period motion in the classical with a selected perturbed case.

We can observe that, from Fig. 5a, and 5b, the eccentricity of the long-period orbit decreases under the effect of the perturbations, while the eccentricity of the short-period one increases. Also, we see from the figures that the perturbed case are shifted from the classical case because of the influence of the disturbing forces. Ignoring all the perturbations considered in the present work, our results will be the same as those obtained by Szebehely, (1967).

7. CONCLUSIONS

In this work, we have investigated the periodic orbits around the triangular libration points $L_{4,5}$, in the range $0 < \mu < \mu_c$. We formulated the problem in a more general way and used a more complex mathematical model than previously published papers that considered the classical case (Abouelmagd and Mostafa, 2015). The prolateness coefficients of both primaries are taken into account as a perturbing force. We investigated the variations of the angular frequencies for the long and the short periodic orbits. The variation of both frequencies is represented graphically versus the mass parameter μ for distinct values of the included perturbations. It is found that for small mass ratio μ , an increment in the perturbing forces results in a decrease in the frequency of the short-period orbit, while an increment in the same parameters will increase the frequency of the long-period one. Both frequencies coincide at the critical value of the mass parameter μ_c . In addition, we derived explicit expressions for the eccentricities e_1 and e_2 of the long and short-period orbits. We represented graphically both eccentricities versus the mass parameter. It is found that the eccentricities e_1 and e_2 of the long and short-period orbits are decreasing and increasing functions, respectively. Furthermore, we studied the orientation of the principle axes of the ellipses. It is observed that the included perturbing forces influence the orientation of the principal axes. The perturbing forces result in a change in the inclination angle of the orbits. Finally, in our opinion, we believe that the current research has special importance to space science applications to send spacecraft into stable regions in planetary systems.

REFERENCES

- Abd El-Salam F. A. (2019) Periodic and degenerate orbits around the equilibrium points in the relativistic restricted three-body problem., *Iranian Journal of Science and Technology, Transactions A: Science*, Vol. 43, No. 1 , 173-192.
- AbdulRaheem A. and Singh J. (2008) Combined effects of perturbations, radiation and oblateness on the periodic orbits in the restricted three-body problem, *Astrophysics and Space Science*, Vol. 317, 9–13.
- Abouelmagd E. I., M. S. Alhothuali, Juan L. G. Guirao, and H. M. Malaikah (2015) Periodic and

Secular Solutions in the Restricted Three–Body Problem under the Effect of Zonal Harmonic Parameters, *Applied Mathematics & Information Sciences*, Vol. 9, No. 4, 1659-1669.

Abouelmagd E. I., Alzahrani. F, Guirou J L. G., Hobiny A. (2016) Periodic orbits around the collinear libration points, *Nonlinear Sci.Appl.(JNSA)*, Vol.9(4:1716-1727

Abouelmagd, E. I. and Mostafa, A. (2015) Out of plane equilibrium points locations and the forbidden movement regions in the restricted three-body problem with variable mass. *Astrophysics and space science*, 357(1), 1-10.

Alrebdi H. I., Papadakis K.E., Dubeibe F. L., and Zotos E. E. (2022) Equilibrium Points and Networks of Periodic Orbits in the Pseudo-Newtonian Planar Circular Restricted Three-body Problem. *The Astronomical Journal*, Vol. 163, No. 2 , 75.

Alrebdi H. I., Smii B., and Zotos E. E. (2022) Equilibrium dynamics of the restricted three-body problem with radiating prolate bodies. *Results in Physics* : 105240.

Beatty J K. , Petersen C. C. and Chaikin A. (1999) The New Solar System, *Cambridge University Press, Cambridge*, 4th edition.

Burgos-García J., Lessard j. p., James J.D. (2019) Spatial periodic orbits in the equilateral circular restricted four-body problem: computer-assisted proofs of existence. *Celestial Mechanics and Dynamical Astronomy* 131.1: 1-36.

Ddvorak R. and Lhotka C. (2013) Celestial Dynamics Chaoticity and Dynamics of Celestial systems, *Wiley-VCH*.

Marsola TCL., da Silva Fernandes, S. , and Balthazar J. M. (2021) Stationkeeping controllers for Earth–Moon L1 and L2 libration points halo orbits. *Journal of the Brazilian Society of Mechanical Sciences and Engineering* 43:347.

Pathak N., Abouelmagd Elbaz I., Thomas V.O. (2019) On higher order resonant periodic orbits in the photo–gravitational planar restricted three–body problem with oblateness. *The Journal of the Astronautical Sciences* 66.4: 475-505.

Kumar P. A. and Sharma D. (2021) Periodic orbits in the restricted problem of three bodies in a three-dimensional coordinate system when the smaller primary is a triaxial rigid body. *Applied Mathematics and Nonlinear Sciences* 6.1 : 429-438.

Radwan M. and Abd El Motelp N. S. (2021) Location and stability of the triangular points in the triaxial elliptic restricted three-body problem., *Revista Mexicana de Astronomia y Astrofisica*, Vol. 57, No. 2, 311–319.

Reiff J., Zatsch J., Main J. and Hernandez R. (2022) On the stability of satellites at unstable libration points of sun–planet–moon systems. *Communications in Nonlinear Science and Numerical Simulation* 104 : 106053.

Saeed T. and Zotos E. E. (2021) On the equilibria of the restricted three-body problem with a triaxial rigid body - I. Oblate primary, *Results in Physics*, Vol. 23, 103990.

Sharma R K. and Jency. A. (2019) Locations of Lagrangian points and periodic orbits around triangular points in the photo gravitational elliptic restricted three-body problem with oblateness, *International Journal of Advanced Astronomy*, Vol. 7, No. 2, 25-38.

Singh J. , Umar A. (2012) On the stability of triangular points in the elliptic R3BP under radiating and oblate primaries, *Astrophysics and Space Science*, Vol. 341, 349–358.

Szebehely V. (1967) Theory of Orbit *Academic Press, New York, 1967*.

Sharma R K. and Subba Rao P V. (1975) Collinear equilibria and their characteristic exponents in the restricted three-body problem when the primaries are oblate spheroids, *Celestial Mechanics*, Vol. 12, 189-201.

Zahra, K., Awad, Z., Dwidar, H. R., Radwan, M. (2017). On stability of triangular points of the restricted relativistic elliptic three-body problem with triaxial and oblate primaries, *Serbian Astronomical Journal*, Issue. 195, 47-52.

Zotos E. E. (2020) Exploring the Planar Circular Restricted Three-body Problem with Prolate Primaries, *Journal of Nonlinear Modeling and Analysis*, <http://jnma.ca>; <http://jnma.ijournal.cn> 2.3 : 411-429.

Received: 2022-05-17

Reviewed: 2022-08-17 (*undisclosed name*); 2022-11-18 (*undisclosed name*);
2023-01-04 (*undisclosed name*)

Accepted: 2023-02-02